

Occluding Junction Structure–Function Relationships in a Cultured Epithelial Monolayer

JAMES L. MADARA* and KIERTISIN DHARMSATHAPHORN*

*Department of Pathology, Brigham and Women's Hospital, Harvard Medical School, and the Harvard Digestive Diseases Center, Boston, Massachusetts 02115; *Department of Medicine, University of California, San Diego, California 92103

ABSTRACT Electrical circuit analysis was used to study the structural development of occluding junctions (OJs) in cultured monolayers composed of T₈₄ cells. The magnitude of the increments in transepithelial resistance predicted by such analysis was compared with the magnitude of the measured increments in resistance. Confluent sheets of epithelial cells were formed after cells were plated at high density on collagen-coated filters. Using Claude's OJ strand count–resistance hypothesis (1978, *J. Membr. Biol.* 39:219–232), electrical circuit analysis of histograms describing OJ strand count distribution at different time points after plating predicted that junctional resistance should rise in a proportion of 1:21:50 from 18 h to 2 d to 5 d. This reasonably paralleled the degree of rise in transepithelial resistance over this period, which was 1:29:59. The ability to predict the observed resistance rise was eliminated if only mean strand counts were analyzed or if electrical circuit analysis of OJ strand counts were performed using an OJ strand count–resistance relationship substantially different from that proposed by Claude. Measurements of unidirectional fluxes of inulin, mannitol, and sodium indicated that restriction of transjunctional permeability accounted for the observed resistance rise, and that T₈₄ junctional strands have finite permeability to molecules with radii ≤ 3.6 Å but are essentially impermeable to molecules with radii ≥ 15 Å. The results suggest that general correlates between OJ structure and OJ ability to resist passive ion flow do exist in T₈₄ monolayers. The study also suggests that such correlates can be obtained only if OJ structural data are analyzed as an electrical circuit composed of parallel resistors.

The intercellular occluding junction (OJ)¹ serves as the rate-limiting barrier that restricts passive diffusion of molecules through the paracellular channel (for reviews, see references 1–3). Initially, data derived from a variety of native unperturbed epithelia led to the view that specific structural aspects of OJs, such as OJ strand counts assessed in freeze-fracture replicas, generally correlate with the ability of epithelia to resist passive transepithelial ion flow (4, 5). However, a comparison of OJ structure and paracellular resistance between the epithelial linings of mammalian ileum and toad bladder failed to support this view (6). There are two potential explanations for such conflicting observations. The first, which seems to be more commonly perceived (3, 7, 8), is that general correlations between OJ strand counts and OJ function at the cellular level do not exist. However, an alternative possibility

is that the methods commonly used to compare OJ structure with measurements of OJ function may, at times, be inappropriate. For example, intestinal epithelium is composed of many cell types that display cell type-specific junctional structure (9) and permeability (10). However, the commonly used parameter of net OJ function, electrical resistance, recognizes the network of tissue OJs as an electrical circuit composed of individual resistors (i.e., individual OJs) arranged in parallel. Since such circuits may be dominated by a low resistance element, even if present at low frequency (11), it follows that a mean value of OJ strand count is a grossly inadequate parameter for comparison with such resistance values. Meaningful interpretation of intestinal OJ structure–function relationships are further complicated by the cell type-specific variations in the amount of OJ per unit surface (linear junctional density) and the profound serosal-to-mucosal surface amplification (11). We have recently

¹ Abbreviation used in this paper: OJ, occluding junction.

shown that analysis of all of the above OJ structural data in terms of an electrical circuit unmasked conserved OJ structure-function relationships between ileal and urinary bladder epithelium (11).

Our goal was to use the above circuit analysis approach to probe OJ structure-function relationships during *de novo* OJ development in a simple system composed of a relatively uniform cell population. Although various key aspects of the cell biology of OJs have been elegantly probed using the simple model of Madin-Darby canine kidney monolayers (12–18), we chose not to use this system since the passages of Madin-Darby canine kidney cells most thoroughly studied develop relatively low transepithelial resistance (80–120 $\Omega \cdot \text{cm}^2$).

We recently found that monolayers of intestinal T₈₄ cells develop transepithelial resistance values of $\sim 1,500 \Omega \cdot \text{cm}^2$. The T₈₄ cell line was established from a human colonic carcinoma and has properties of a functionally well-differentiated Cl⁻-secreting cell (19, 20). Furthermore, the stoichiometry and alignment of the various transporters and channels that participate in Cl⁻ secretion are similar between T₈₄ cells (20) and the Cl⁻-secreting crypt cells of the intact intestine (21, 22). Using a circuit analysis type of approach, we use this model to sequentially analyze OJ structure during monolayer development, and verify that the progressive rise in transepithelial resistance specifically reflects a progressive restriction of passive transjunctional permeability.

MATERIALS AND METHODS

Cell Culture: T₈₄ cells (19) were grown as monolayers in a 1:1 mixture of Dulbecco-Vogt modified Eagle's medium and Ham's F-12 medium supplemented with 15 mM Na⁺-HEPES buffer, pH 7.5, 14 mM Na HCO₃, 40 mg/liter penicillin, 8 mg/liter ampicillin, 90 mg/liter streptomycin, and 5% newborn calf serum (19). For subcultures, a cell suspension was obtained from confluent monolayers by exposing the latter to 0.1% trypsin and 0.9 mM EDTA in Ca²⁺- and Mg²⁺-free phosphate-buffered saline (19). To prepare monolayers of cells for experimental purposes, T₈₄ cells were grown on collagen-coated permeable supports which could be inserted into modified Ussing chambers without trauma to the monolayers, as previously described (19). Nucleopore filters (5- μM pore) were coated on one side with rat tail collagen (23). These collagen-coated filters were subsequently glued to one end of Lexan rings and sterilized. The resulting "wells," which now had a 1.98-cm² collagen-coated filter as their base, were plated with 10⁶ T₈₄ cells. These ring-mounted collagen supports were then cultured in dishes for periods of from 18 h to 16 d in the above medium under conditions that elevated them from the bottom of the plastic culture dish, thus allowing the basolateral surface ready access to the nutrient culture media (19, 24). 116 monolayers, representing cells in passages 27–34, were used for these experiments.

Ussing Chamber Studies: At designated intervals after T₈₄ cells were plated on ring-mounted collagen supports, the rings were removed from the culture media and inserted into modified low turbulence Ussing chambers (19). Individual monolayers were used only once. The inserted monolayers separated the Ussing chamber into two reservoirs that contained identical volumes of continually stirred and oxygenated solution (pH 7.4, 37°C) containing (millimolar): Na, 140; K, 5.2; Ca, 1.2; Mg, 1.2; Cl, 119.8; HCO₃, 25; MgPO₄, 2.4; HPO₄, 0.4; and glucose, 10. Each reservoir was connected via agar bridges to voltage-sensitive calomel electrodes and to Ag-AgCl current-passing electrodes, which were positioned to ensure a uniform current density at the monolayer interface. Voltage deflections elicited by passage of defined current pulses were used to determine transepithelial resistance. After equilibration, resistance was measured and recorded as the absolute resistance minus the fluid resistance. The resistance of the collagen-coated Nucleopore filter was neglected since it was found to be insignificant ($<3 \Omega \cdot \text{cm}^2$).

For determination of flux rates of mannitol or inulin across maturing T₈₄ monolayers, multiple sets of monolayers of different age were used. Flux experiments were performed under short-circuit conditions. 5 μCi of either [³H]mannitol or [³H]inulin was added to one reservoir; both reservoirs contained either 5 mM mannitol or 1 mM inulin added to the glucose buffer solution. For each age group assayed, unidirectional flux rates were determined

with monolayer pairs in which resistance differed by no more than 10% (22).

Morphologic Techniques: After removal from the modified Ussing chambers, the monolayers were immediately submerged in a fixative at 4°C and pH 7.4. For thick and thin section study the fixative predominantly used was 2% glutaraldehyde in 0.1 M Na cacodylate buffer. After 1 h, tissues were rinsed in cacodylate buffer, postfixed in 1% OsO₄ for 1 h, dehydrated through graded alcohols, and embedded in epoxy resin. Oriented 1- μm sections were obtained with glass knives, and, to judge monolayer confluence at high resolution, multiple areas were thin sectioned, mounted on copper mesh grids, and stained with uranyl acetate and lead citrate.

For freeze-fracture the cells were fixed with 2% freshly prepared formaldehyde, 2.5% glutaraldehyde in 0.1 M Na cacodylate, pH 7.4, for 1 h at 4°C. After fixation, monolayers were removed from the collagen support with a rubber policeman. The resulting sheets of epithelium were processed for freeze fracture (11). Specimens were fractured at a stage temperature of -110°C in a Balzers 300 freeze-etch device (Balzers, Hudson, NH) and were replicated, cleaned, and examined as previously described (11).

Quantitative evaluation of OJ structure was carried out in monolayers 18 h, 2 d, and 5 d after plating. 17 replicas selected on the basis of quality were used for these studies and evaluated for OJ strand count as previously described (25).

Circuit Analysis of Structural Data: To interpret the functional meaning of OJ strand counts with regard to their ability to resist passive ion flow, we analyzed structural data as one would analyze an electrical circuit using the following relationship (11): $(1/R_T) = (1/R_1)(F_1) + (1/R_2)(F_2) + \dots + (1/R_x)(F_x)$, where R_T is the total circuit resistance, $R_{1,2,\dots}$ is the resistance of individual resistors (OJs), and F is the frequency of each specific type of resistor in the circuit. This approach tested Claude's OJ strand count-resistance hypothesis since R values for individual OJ strand counts were obtained from Claude's graph (5) that correlates junctional resistance, corrected for variations in junctional linear density, with junctional strand counts over a broad range of epithelia. Thus, for each category of strand count obtained, a corresponding resistance value was read directly from Claude's graph to obtain the R values for the above equation. R values corresponding to 0 strand counts from the graph were used for strand counts corresponding to sites in which no well-developed strand was observed but in which a particle-lined ridge suggestive of a forming strand was identified. This maneuver assumes that the rate-limiting barrier at such sites is not the particle-lined ridge but the physical restraint of close apposition between the lateral membranes of adjacent cells. Such R values would be inappropriate to use for our strand counts for 0, however, since we show that separations of ~ 100 – 300 nm may exist at sites of OJ discontinuity. The resistance of the intercellular space at sites of restriction varies inversely with the width of the separation (5). If the physical restriction at the site of an incompletely developed strand is ~ 1 nm, then the resistance due to physical restriction of these 100–300-nm spaces should be diminished by approximately two orders of magnitude. Therefore, strand counts of 0 were given resistance values two orders of magnitude below those of developing strands with particle-lined ridges. R_T 's were then calculated for each of the three groups in which OJ strand counts were quantitated, and these three values were expressed as relative proportions.

We also corrected the above, calculated values of predicted resistance for variations in linear junctional density² that occur from day 2 to day 5 monolayers. Thin sections ($n = 6$), taken both from 2- and 5-d monolayers were morphometrically analyzed for junctional densities by methods previously described (7), and results were expressed as meters of occluding junction per square centimeter monolayer surface. We did not attempt to measure linear junctional density in 18-h "monolayers" due to the confounding features of their surface geometry and since they were only 1.25 d removed from the 2-d measurements.

RESULTS

Structural Development of T₈₄ Monolayers

GENERAL

Examination of thick sections obtained from T₈₄ sheets fixed 18 h after plating failed to reveal foci of epithelial discontinuities. These early "confluent" sheets did show great heterogeneity in the shape of individual cells as well as in cell stacking (Fig. 1). Thin sections from 18-h sheets revealed

² Linear junctional density is the amount of junctional length per unit of epithelial surface and is dependent on the apical diameter and contour of epithelial cell plasma membranes.

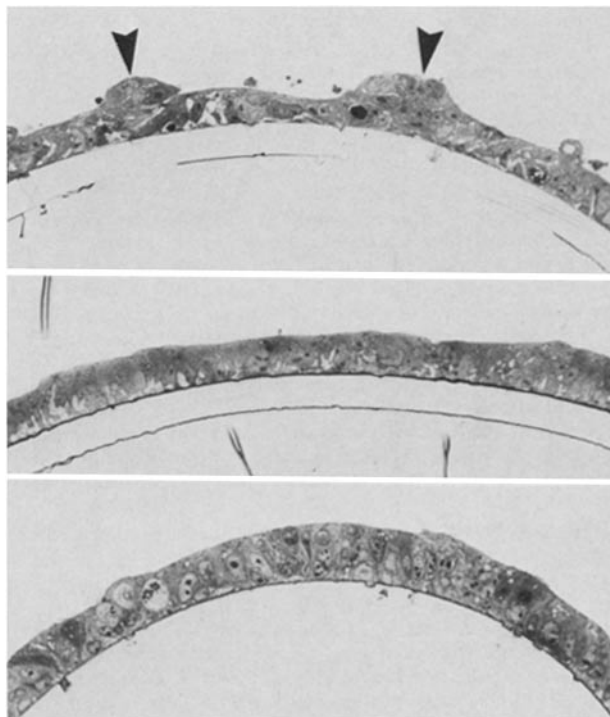


FIGURE 1 1- μ m sections of T₈₄ epithelial sheets 18 h (top), 2 d (middle), and 5 d (bottom) after plating 10⁶ cells on collagen-coated Nucleopore filters (2-cm² surface area). At 18 h, although confluent by light microscopy, true monolayers are not formed, and occasional multilayered foci (arrowheads) are observed. Thin section of such multilayered areas revealed belt-like OJs associated with only the uppermost cells. Progressive differentiation toward true confluent monolayers composed of taller, polarized cells occurs from 2 to 5 d. $\times \sim 200$.

apical membranes containing microvilli 0.1–0.3 μ m long, whose density varied greatly from cell to cell. With further development T₈₄ cell shape became less heterogeneous and by day 2 monolayers of cuboidal epithelial cells were formed (Fig. 1). Monolayers were composed of low columnar cells by day 5 (Fig. 1).

OJs

Analysis of occluding junction structure focused on monolayers from three time points: 18 h, 2 d, and 5 d after plating.

18 H: Although cultures were confluent as judged by 1- μ m sections, at 18 h thin sections revealed occasional 0.1–0.3- μ m gaps between adjacent epithelial cells in which OJs were focally absent. Such sites were also identified in freeze-fracture replicas since well-developed microvilli served to distinguish the apical membrane from the basolateral membrane, which either is smooth or displays the broad folds of nascent interdigitations (Fig. 2). Quantitative freeze-fracture data (Fig. 3) revealed that $\sim 2\%$ of OJ sites from 18-h cultures displayed no strands (Fig. 3), and $\sim 10\%$ of the OJs were composed of a single fine intramembrane particle-lined ridge instead of continuous strands or grooves (Figs. 3 and 4). Approximately 10% of OJs had only a single well-formed strand (Fig. 3). The remaining 18-h OJs had variable strand counts (Fig. 3), which were a result of structural heterogeneity both between and within (Fig. 5) individual OJs. The mean OJ strand count at 18 h was 4.03 ± 0.22

Thin sections in regions of multilayered cells showed that

the deeper cells, unlike the surface cells, did not have apical OJ zones but did occasionally have small lumena between them that were surrounded by plaques of junctional elements and thus were similar to “secondary lumena” seen during fetal gut development (26, 27).

2 D: 2 d after plating, no OJ discontinuities could be found by thin section or by freeze-fracture. Particle-lined ridges represented $<2\%$ of OJ strand counts and strand counts of one accounted for $<5\%$ of the total (Fig. 3). The mean strand count for these monolayers was 4.22 ± 0.20 . Linear junctional density at 2 d was 19.6 m OJ per cm² of monolayer surface.

5 D: Thin sections obtained from monolayers after 5 d revealed OJ zones that appeared more uniform in depth than those at earlier times (Fig. 6). Freeze-fracture images of OJs revealed relatively uniform strand composition within single OJs although strand composition was still somewhat variable between OJs (Fig. 7). Less than 5% of OJ strand counts were <3 (Fig. 3), and the mean strand count was 5.51 ± 0.19 . Strands composed of T₈₄ OJs often ran closely parallel to one another (Fig. 5). Linear junctional density was 30.8 m OJ per cm² monolayer surface at 5 d.

Ussing Chamber Studies

The development of transepithelial resistance with time after plating was initially determined using 48 monolayers. At 18 h monolayers had a mean resistance of $<29 \Omega \cdot \text{cm}^2$ (Fig. 8). Resistance progressively rose from this level to $\sim 1,500 \Omega \cdot \text{cm}^2$ by 5 d (Fig. 8).

Flux data demonstrated that maximal restriction of inulin permeability occurred by the time resistance had achieved values slightly greater than $100 \Omega \cdot \text{cm}^2$ (Fig. 9). Mannitol fluxes, however, were incrementally diminished with increasing resistance even after the initial phase occurring between resistances of 20 and 120 $\Omega \cdot \text{cm}^2$ in which progressive mannitol restriction was comparatively large (Fig. 9). Unidirectional flux data showed no significant difference between the rates of flux in the mucosa-to-serosa and the serosa-to-mucosa directions at any monolayer age or with either tracer (Table I). In separate experiments, sodium fluxes were measured to determine if progressive sodium restriction accompanied OJ structural development at higher levels of resistance. As seen in Fig. 10, the rate at which Na⁺ restriction increased as resistance rose was relatively constant. Such Na⁺ movement correlated inversely with monolayer resistance ($r = 0.85$, $P < 0.005$ by least squares). In contrast to mannitol and inulin, Na⁺ may permeate the transcellular as well as the paracellular route. However, because variation in measured parameters of transcellular transport do not vary between 2- and 5-d monolayers (Dharmasathaphorn, K., unpublished observation), this restriction of Na⁺ is probably due to a restriction in paracellular permeability.

Circuit Analysis of Structural Data

The OJ structural data were analyzed as an electrical circuit using the OJ structure–function relationship proposed by Claude (5) (see Materials and Methods). For the three groups of monolayers used for these studies, the predicted proportional increase in resistance uncorrected for variation in linear junctional density was 1:21:71 (for 18 h/2 d/5 d). With correction for the linear junctional density measurements, the

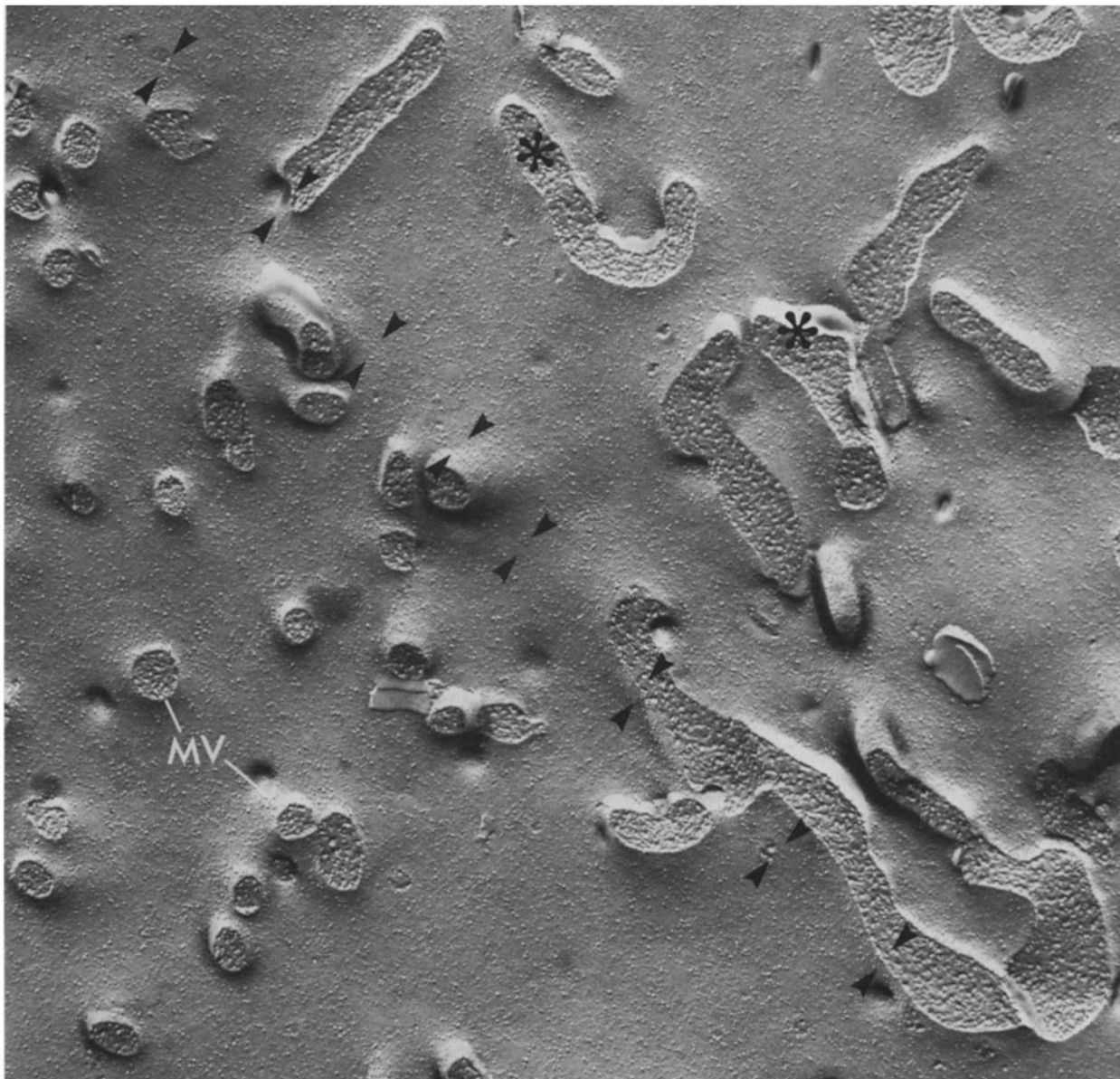


FIGURE 2 Freeze-fracture image of the interface of an apical membrane and a lateral membrane of a T_{84} epithelial cell 18 h after plating. The apical membrane contains multiple cross-fractured microvilli (MV) whereas the lateral membrane has no microvilli but displays broad folds (asterisks) representing nascent lateral interdigitations. The appropriate location for the future site of an OJ is marked with arrowheads. $\times 43,000$.

predicted proportional increase was 1:21:50 and the measured proportional increase in resistance was 1:29:59. Comparing predicted with measured resistance increments at each interval showed corresponding values of 20 vs. 28 times for the first interval (18 h–2 d) and 29 vs. 30 times for the second interval (2–5 d).

In contrast to the ability of circuit analysis to predict the resistance rise, the sequential rises in mean OJ strand count were +0.19 strands and +1.29 strands at 2 and 5 d, respectively, whereas the sequential rises in resistance were $559 \Omega \cdot \text{cm}^2$ and $613 \Omega \cdot \text{cm}^2$.

DISCUSSION

After plating, T_{84} monolayers develop high transepithelial resistance over a 5-d period. Our data strongly suggest that this resistance rise is due to changing paracellular, not trans-

cellular, permeability since this increase is paralleled by a progressive restriction in transepithelial flux of the extracellular space markers inulin and mannitol. The diminished flux of these molecules across T_{84} monolayers with time can not be attributed to transcytosis since they were differentially restricted in accordance with their hydrodynamic radii (mannitol, 3.6 \AA ; inulin, $11\text{--}15 \text{ \AA}$). Since the OJ is the rate-limiting barrier to permeation through the paracellular channel (3), the observed resistance rise is specifically attributable to altered permeability at this anatomical site.

Maximal restriction of inulin flux across the monolayers coincided with the loss of structurally discontinuous OJs. However, many OJ sites displaying one or two strands were still present when inulin flux became restricted, which suggests that a single intact strand is sufficient to impede the passive transjunctional flow of polar molecules $\geq 11\text{--}15 \text{ \AA}$ in hydrodynamic radius. In contrast, whereas an initial rapid phase of

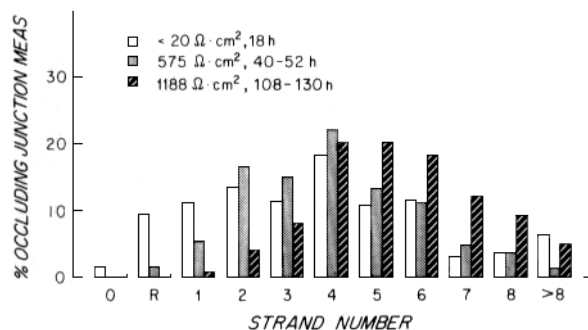


FIGURE 3 Histogram comparing occluding junction strand counts obtained from monolayers at 18 h, 2 d, and 5 d after plating. The most striking feature is the progressive shift, with time, away from junctions with zero, one, or two strands or incompletely developed, single-particle-lined ridges (R). The resistance values represent the mean values for the three groups of epithelial sheets used for these structural studies.



FIGURE 4 Freeze-fracture image of an interface between apical (A) and lateral (L) membranes of a T_{84} epithelial cell 18 h after plating. Occasionally, linear particle arrays (R) occupied the site of the OJ and were often associated with a subtle membrane ridge. Such particulate junctions are comparable to those reported during *de novo* junctional strand formation in a variety of epithelia during fetal development.

progressive mannitol exclusion also coincided with closure of discontinuous OJs, this was followed by a slower phase of progressive restriction of mannitol flux which paralleled a major rise in transepithelial resistance. These data suggest that passive mannitol flux may occur across structurally continuous T_{84} OJs and that progressive restriction of passive transjunctional ion flow is accompanied by progressive restriction of passive transjunctional mannitol flux. These data are comparable to those observed in native intestinal epithelium in which restriction of transepithelial mannitol flux has been shown to parallel restriction of passive paracellular ion movement (28, 29).

Sequential analysis of OJ strand counts during the development of monolayer resistance allowed us to assess if OJ structure-function relationships approximated the strand count-resistance relationship originally proposed by Claude

(5). Using her proposed relationship, we found a reasonable correlation between OJ strand count and resistance to exist if we analyzed our structural data as an electrical circuit composed of parallel resistors (7). Such a structure-function relationship was not revealed if mean values of structure and functional were compared.

The impact of analyzing OJ structure-function relationships using electrical circuit models can be appreciated more fully by arbitrary manipulation of a model electrical circuit (epithelium) containing 100 parallel resistors (OJs). As shown in Table II, net circuit transjunctional resistance is markedly influenced by low resistance pathways even if such pathways are present at low frequency. For example, circuit 4 differs from circuit 3 only by the substitution of two resistors with resistances of $10^2 U$ for two resistors with resistances of $10^4 U$. Due to the low frequency of this substitution, the mean resistance of components of the two circuits is comparable. However, the net resistance across these two circuits varies by more than one order of magnitude. In contrast, as is evident from comparing circuit 2 with circuit 1, high frequency substitution with components of lower resistance results not only in lower circuit resistance but also in lower mean component resistance. Thus, in contrast to the comparison between circuits 3 and 4, the functional result of this manipulation can be readily detected by measurements of mean component function (or of a structural parameter that relates to mean component function). These circuit models demonstrate the following principle, which impacts on the study of OJ structure-function relationships: When OJ heterogeneity exists, mean values of OJ structure or function may not correlate well with the net behavior of the population. A documented example of this principle comes from elegant microelectrode surface scanning studies of Madin-Darby canine kidney cells. The Madin-Darby canine kidney monolayers used for these studies had low overall resistance; however, current sinks were only localized at a minor subpopulation of intercellular junctions (14). Those authors also documented different OJ populations with respect to strand counts and proposed that the minor OJ population with only one or two junctional strands corresponded to the sites of current sinks that dominated the behavior of this model epithelium (14).

This study of OJ development in T_{84} monolayers, as well as other studies of a variety of unperturbed epithelia (1, 2, 4, 5, 10, 11, 30, 31), suggest that OJ structure-function relationships do exist. These data also suggest that the specific OJ structure-function relationship present in these diverse epithelia approximate that originally proposed by Claude: OJ strand counts correlate positively with the log of paracellular resistance (5). If exceptions to this general relationship exist we do not feel they have yet been reasonably documented. Studies widely cited as exceptions to the above OJ structure-function relationship in unmanipulated epithelia (6) often predate the recognition of the need for an electrical circuit analysis approach. They also failed to consider other key issues such as variation in linear junctional density or differences in serosal-to-mucosal surface area enrichment. Other frequently cited studies that fail to show OJ structure-function relationships in unperturbed, but developing, epithelia often deal with systems that are difficult to understand with precision. For example, studies of developing fetal sheep choroid plexus epithelium show little change in mean OJ structure, whereas the plasma to cerebral spinal fluid flux of intervase-

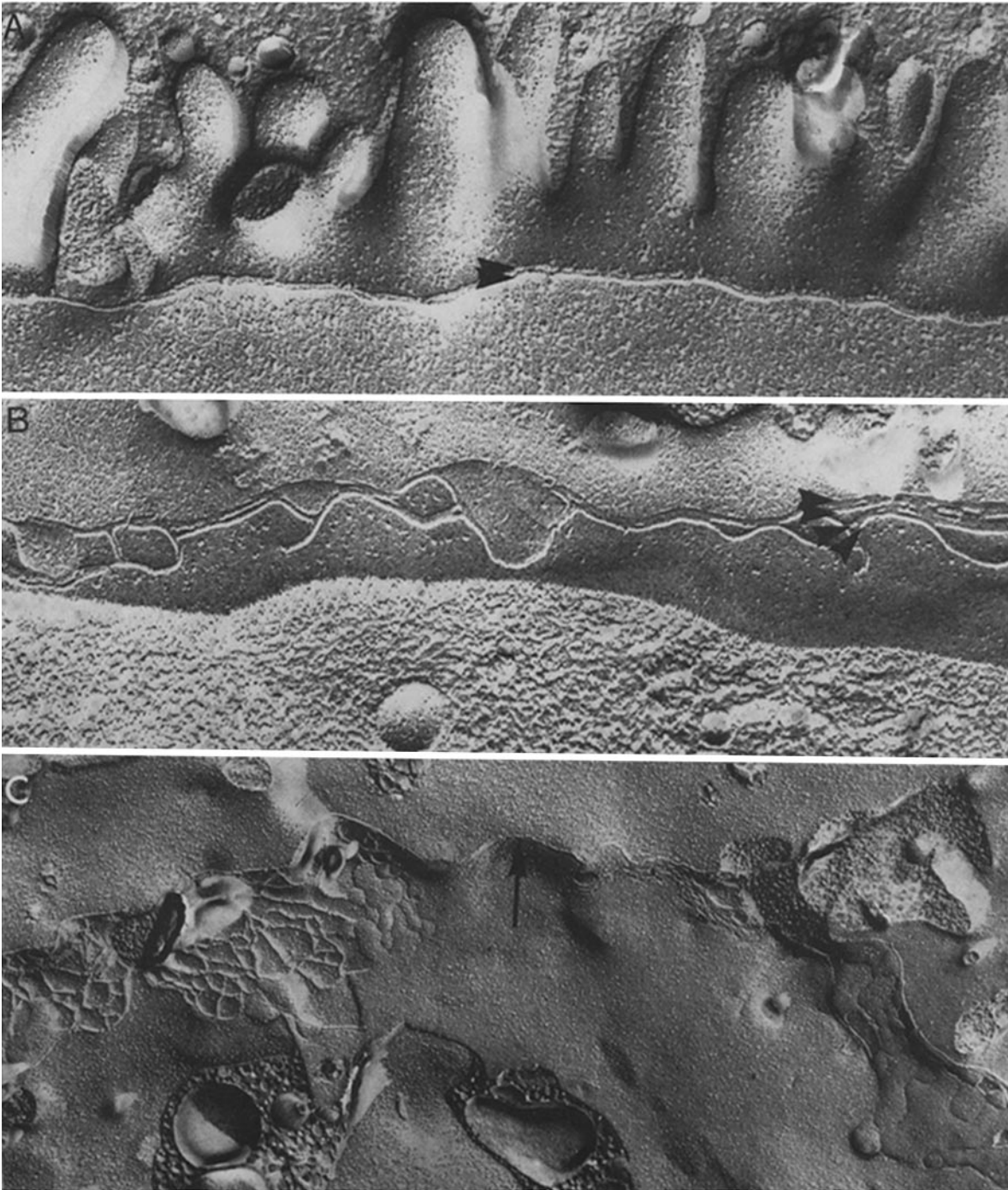


FIGURE 5 Freeze-fracture images of continuous occluding junctions in T_{84} epithelial cells 18 h after plating. Variation in numbers of OJ strands is marked both between (A, B) and within (C) junctions. (A) 18-h OJs appearing as a simple duplex of two closely apposed strands (arrowheads). (B) T_{84} junctional strands focally and frequently occurred as two to five closely apposed strands with little if any interstrand space (arrowheads). (C) Extreme variation in the numbers of strands within a single occluding junction could frequently be observed when large continuous expanses of junction were revealed. Thus junctions with areas composed of four to eight intermeshed strands could also contain substantial lengths composed of only one or two strands (arrow). The direction of shadow in A and B is approximately from top to bottom. For C the direction of shadow is approximately from bottom to top. (A-C) $\times 90,000$; $\times 81,000$; $\times 45,000$.

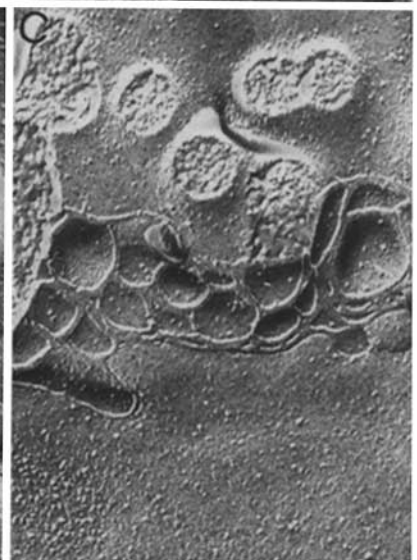
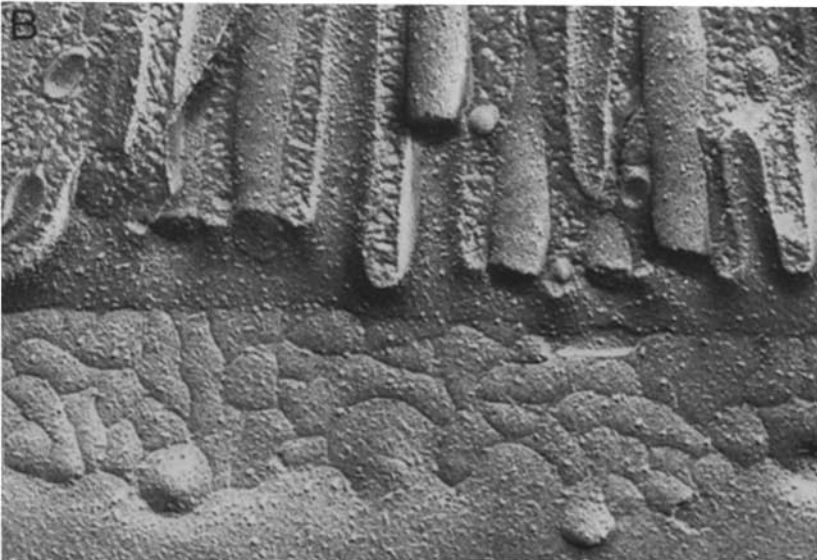
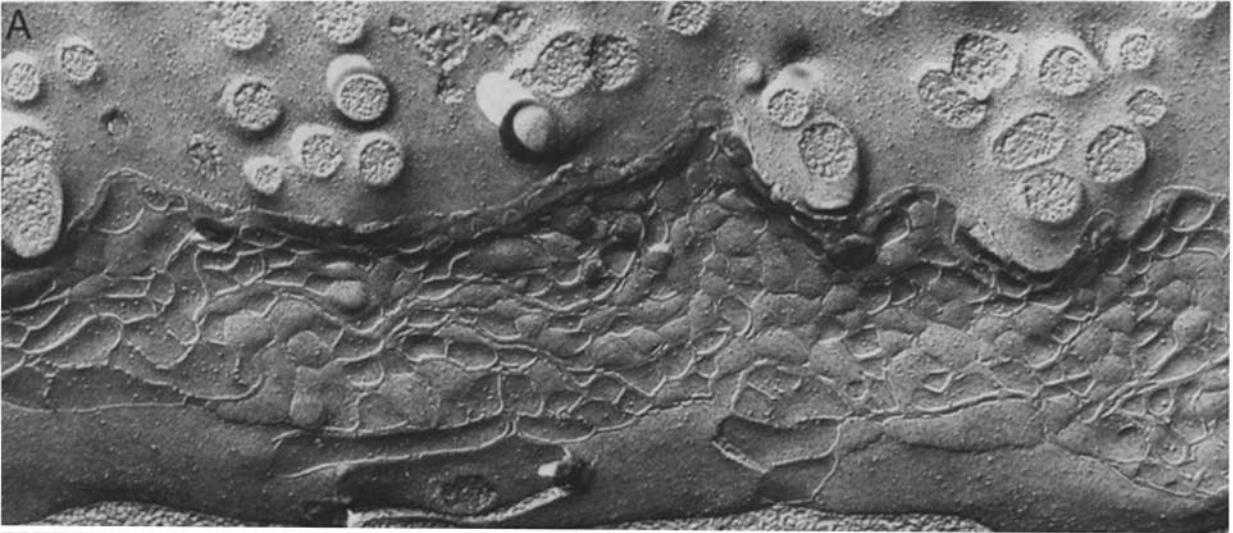
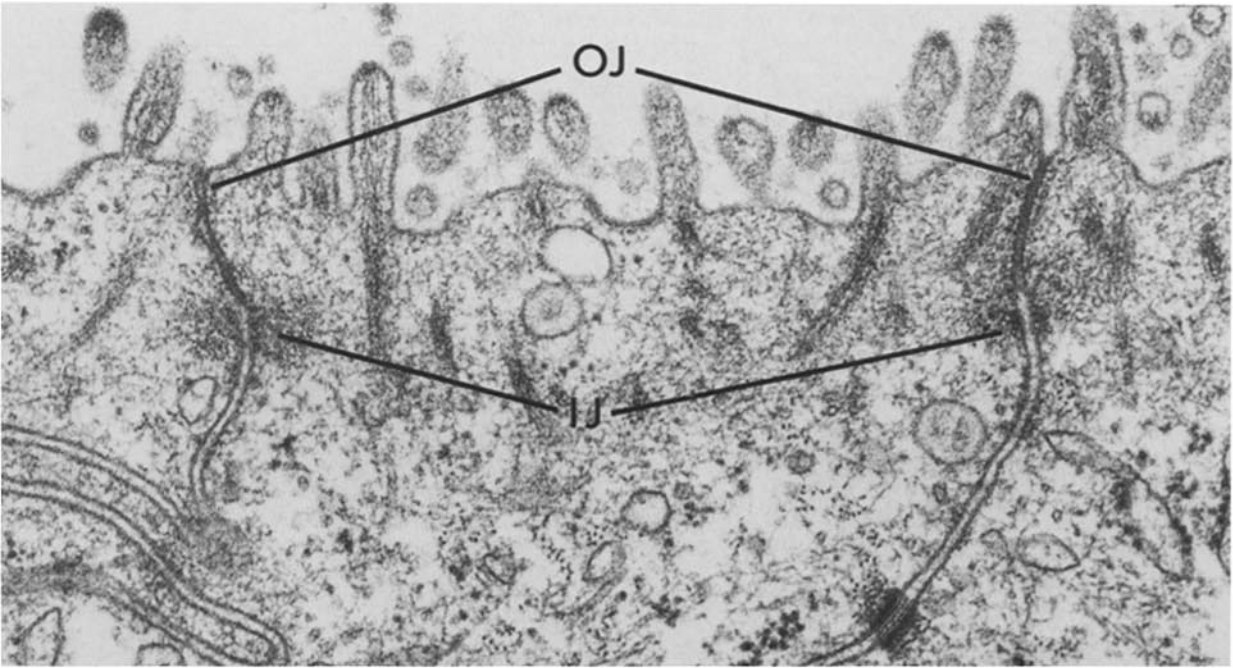


TABLE I. Unidirectional Flux of Inulin and Mannitol Across T_{84} Monolayers of Varying Resistance

Resistance $\Omega \cdot \text{cm}^2$	j_{inulin}		j_{mannitol}	
	ms	sm	ms	sm
	$\mu\text{mol/h} \cdot \text{cm}^2$			
30 ± 7	0.010 ± 0.001	0.014 ± 0.002	0.398 ± 0.041	0.395 ± 0.040
128 ± 7	0.001 ± 0.0002	0.002 ± 0.0004	0.058 ± 0.004	0.062 ± 0.006
531 ± 88	0.003 ± 0.003	0 ± 0	0.028 ± 0.015	0.013 ± 0.005

The junctional restriction in tracer (j) is independent of the direction in which flux is measured (ms, mucosa-to-serosa direction, sm, serosa-to-mucosa direction). These data further highlight the early maximal restriction that occurs for inulin, but not for mannitol, flux.

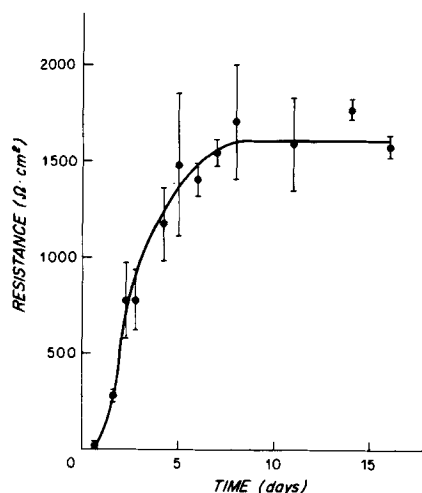


FIGURE 8 Progressive rise in T_{84} monolayer resistance to passive ion flow with time. Although confluent by light microscopy 18 h after plating, monolayers have minimal resistance at this time. Resistance progressively rises in the ensuing 5-d period to stabilize at values of $\sim 1,500 \Omega \cdot \text{cm}^2$.

cularly injected, labeled hydrophilic molecules changes dramatically over the same time course (32). However, measurements of resistance could not be obtained, cerebral hemisphere capillary density and choroid plexus surface area changed during this time and doubled in weight, and there was no way to exclude the potential for passive flux of intravascular markers into the cerebral spinal fluid by way of the ependyma (32). Many similar uncertainties are present in comparable studies of fetal lung development (33). In another study of fetal choroid plexus development which is cited to debunk the notion of an OJ structure-function relationship the authors argue that a transepithelial shunt of macromolecules occurring at an early but not a late fetal stage is via a transcellular, not a paracellular, route (34). If the latter interpretation is correct, this study is irrelevant to the issue of OJ structure-function relationships.

Other data suggest that OJ structure-function relationships can be altered experimentally. Martinez-Palomo and Erlj (6)

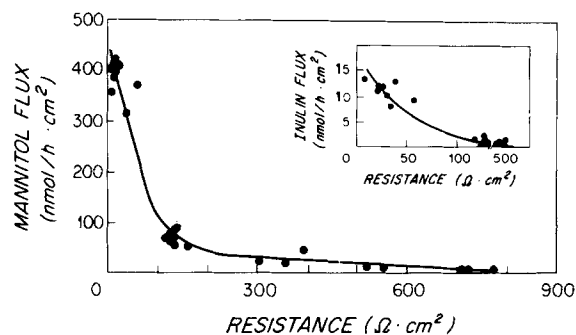


FIGURE 9 Transjunctional serosal-to-mucosal flux rates of the extracellular space markers mannitol (main graph) and inulin (inset) from the apical bath to the basolateral bath. Flux rates of inulin and mannitol decline substantially as resistance approaches values exceeding $100 \Omega \cdot \text{cm}^2$, the value that corresponds to the period in which discontinuous junctions became continuous. Inulin flux is maximally restricted at this time of OJ "closure," whereas mannitol flux progressively declines as resistance continues to rise to values of $500 \Omega \cdot \text{cm}^2$.

have shown that the decrease in toad bladder transepithelial resistance elicited with hypertonic urea solutions produces a simplification of OJ structure. However, treatment of this epithelium with hypertonic lysine solutions produced the functional, but not the structural, alteration in OJs (6). Although circuit analysis of the OJ structural data was not performed, lanthanum tracer experiments showed that $>90\%$ of OJs were permeabilized and suggested that the OJ functional defect occurred throughout this epithelium (6). It is unclear why such discrepancies exist. One possibility suggested to us by a reviewer of this manuscript is that OJ strands of individual cells detach from those of neighboring cells, producing a fall in resistance, without a change in strand count. In contrast to the above example, parallel alterations in OJ structure and function have been observed in a variety of other manipulated systems. We have shown that the expansion of jejunal absorptive cell OJ structure elicited by short-term mucosal osmotic loads is accompanied by an increase in resistance as well as by a preferential restriction of the transjunctional passive movement of cations (25). Similar

FIGURE 6 Thin section appearance of occluding junctions from monolayers 5 d after plating. The appearance of OJs became relatively uniform in thin sections by 5 d. Junctional organization was also characterized by the ordered relationships between occluding junctions and underlying intermediate junctions (l/l). $\times 32,000$.

FIGURE 7 Freeze-fracture images of OJs from T_{84} monolayers 5 d after plating. (A) OJs that display high strand counts throughout their length constitute a minor junctional population. Although presumably of extremely high resistance, overall such junctions would contribute insignificantly to measurements of monolayer resistance. (B and C) The major population of junctions have substantially fewer strands than that shown in A and are uniform and regularly composed of three to five grooves or strands. $\times 64,000$.

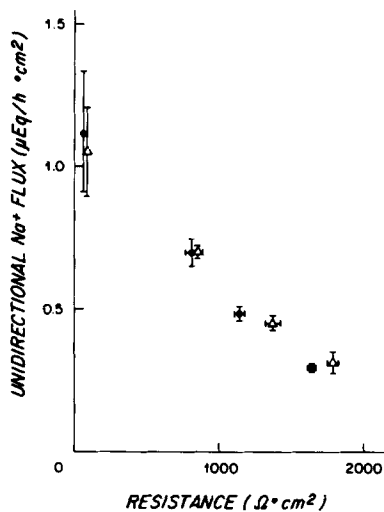


FIGURE 10 Transepithelial serosal-to-mucosal (circles) and mucosal-to-serosal (triangles) flux rates of Na^+ . Passive transepithelial Na^+ flux is restricted progressively with increasing resistance and is equally restricted in both directions. The decrease in flux rate per unit of increment in resistance appears linear over this broad range, and, since parameters of transcellular transport do not change from day 2 to day 5, it supports the notion that such restriction primarily represents a decrease in passive paracellular ion flow.

TABLE II. Analysis of OJs as a Parallel Electrical Circuit: Effects of Manipulation of Resistance Values in an Imaginary Epithelium Composed of 100 Resistive Junctions (R_1 - R_{100})

Circuit	Resist-	Mean compo-	Resistance
	ance of		
	components		
	U	U	U
1. R_{1-100}	10^6	10^6	10^4
2. R_{1-50}	10^6	5.5×10^5	1.8×10^3
	R_{51-100}		
	10^5		
3. R_{1-50}	10^6	5.4×10^5	6.9×10^2
	R_{51-90}		
	10^5		
	R_{91-100}		
	10^4		
4. R_{1-50}	10^6	5.4×10^5	4.7×10^1
	R_{51-90}		
	10^5		
	R_{91-98}		
	10^4		
	R_{99-100}		
	10^2		

The specific values for individual resistors that are used in the above comparison (i.e., 10^4 - 10^6 U) were selected since they correspond to the range of estimated junctional resistance values for OJ strand counts that commonly occur in various epithelia (one to seven strands) (5). The minor value used in circuit 4 (10^2 U) corresponds to the junction resistance value that would approximate that of an "OJ" that had no strands but was the site at which the lateral membranes of adjacent cells were separated by a space tenths of micrometers in dimension (see Results for derivation and see text for discussion of these model circuits as they relate to analysis of occluding junction structure-function relationships). These model circuits are arbitrarily manipulated and do not represent the specific data presented in Results.

OJ structural alterations have accompanied resistance increases in gallbladder epithelium exposed to cyclic AMP (35), plant cytokinins and cytochalasins (36), and the calcium ionophore A23187 (37). Conversely, depletion of Ca^{++} results in a decrease in OJ strand count and transepithelial resistance (37).

Whereas an extensive literature has served as the basis for the formulation of the hypothesis (4, 5) relating OJ structure to OJ ion barrier function, the literature regarding OJ structure-OJ macromolecular barrier function is more limited. OJ

strand discontinuities have been found in perturbed (38) and unperturbed (39) epithelia that leak macromolecules. However in other models of induced transjunctional permeability to macromolecules such OJ strand gaps were not identified (40-42), although junctional structure was simplified and transepithelial resistance was diminished (41). These data suggest that defects allowing macromolecular penetration can be introduced into "normal" strands without introducing complete discontinuities detectable by routine freeze fracture techniques. However, our data suggest that during *de novo* formation of OJs, their ability to exclude molecules substantially larger than mannitol coincides with the development of continuous OJ strands.

We express our gratitude to Drs. James McRoberts and Kenneth Mandel (Department of Medicine, University of California) for their invaluable aid and advice, and to Susan Carlson (Department of Pathology, Brigham and Women's Hospital, Harvard Medical School), Dianna Picton (Department of Pathology, Brigham and Women's Hospital, Harvard Medical School), and Greg Beuerlein (Department of Medicine, University of California) for their expert technical support. Finally, we thank Mary LoGiudice for typing and editing the manuscript.

This work was supported by National Institutes of Health grants AM35932 and AM28305. Dr. Madara is supported in part by the American Gastroenterological Association/Ross Research Scholar Award, and Dr. Dharmasathaphorn is supported in part by the American Gastroenterological Association/Galaxo Research Scholar Award.

Received for publication 1 May 1985, and in revised form 17 August 1985.

REFERENCES

- Madara, J. L., and M. Marcial. 1984. Structural correlates of intestinal tight junction permeability. In *Mechanisms of Intestinal Electrolyte Transport and Regulation by Calcium*. M. Donowitz and G. W. B. Sharp, editors. Alan R. Liss Inc., New York. 77-100.
- Neutra, M. R., and J. L. Madara. 1982. The structural basis of intestinal ion transport. In *Fluid and Electrolyte Abnormalities in Exocrine Glands in Cystic Fibrosis*. P. M. Quinton, J. R. Martinez, and U. Hopfer, editors. San Francisco Press, San Francisco. 194-226.
- Powell, D. W. 1981. Barrier function of epithelia. *Am. J. Physiol.* 241:G275-G288.
- Claude, P., and D. A. Goodenough. 1973. Fracture faces of zonulae occludentes from "tight" and "leaky" epithelia. *J. Cell Biol.* 58:390-400.
- Claude, P. 1978. Morphological factors influencing transepithelial permeability: a model for the resistance of the zonula occludens. *J. Membr. Biol.* 39:219-232.
- Martinez-Palomo, A., and D. Erlij. 1975. Structure of tight junctions in epithelia with different permeability. *Proc. Natl. Acad. Sci. USA.* 72:4487-4491.
- Erlij, D. 1982. Discussion. In *The Paracellular Pathway*. S. E. Bradley and E. F. Purcell, editors. Josiah Macy, Jr. Foundation, New York. 31.
- Bullivant, S. 1982. Tight junction structure and development. In *The Paracellular Pathway*. S. E. Bradley and E. F. Purcell, editors. Josiah Macy, Jr. Foundation, New York. 18.
- Madara, J. L., J. S. Trier, and M. R. Neutra. 1980. Structural changes in the plasma membrane accompanying differentiation of epithelial cells in human and monkey small intestine. *Gastroenterology.* 78:963-975.
- Madara, J. L., and J. S. Trier. 1982. Structure and permeability of goblet cell tight junctions in rat small intestine. *J. Membr. Biol.* 66:145-157.
- Marcial, M. A., S. L. Carlson, and J. L. Madara. 1984. Partitioning of paracellular conductance along the ileal crypt-villus axis: a hypothesis based on structural analysis with detailed consideration of tight junction structure function relationships. *J. Membr. Biol.* 80:59-70.
- Martinez-Palomo, A., I. Meza, G. Beady, and M. Cerejido. 1980. Experimental modulation of occluding junctions in a cultured transporting epithelium. *J. Cell Biol.* 87:736-745.
- Griep, E. B., W. J. Dolan, E. S. Robbins, and D. D. Sabatini. 1983. Participation of plasma membrane proteins in the formation of tight junctions by cultured epithelial cells. *J. Cell Biol.* 96:693-703.
- Cerejido, M., E. Stefani, and A. Martinez-Palomo. 1980. Occluding junctions in a cultured transporting epithelium: structural and functional heterogeneity. *J. Membr. Biol.* 53:19-32.
- Cerejido, M., I. Meza, and A. Martinez-Palomo. 1981. Occluding junctions in cultured epithelial monolayers. *Am. J. Physiol.* 240:C96-C102.
- Meza, I., G. Ibarra, M. Sabanero, A. Martínez-Palomo, and M. Cerejido. 1980. Occluding junctions and cytoskeletal components in a cultured transporting epithelium. *J. Cell Biol.* 87:746-754.
- Gonzalez-Mariscal, L., B. Chavez de Ramirez, and M. Cerejido. 1984. Effect of temperature on the occluding junctions of monolayers of epithelioid cells (MDCK). *J. Membr. Biol.* 79:175-184.
- Meza, I., M. Sabanero, E. Stefani, and M. Cerejido. 1982. Occluding junctions in MDCK cells: modulation of transepithelial permeability by the cytoskeleton. *J. Cell. Biochem.* 18:407-421.

19. Dharmasathaphorn, K., K. G. Mandel, J. A. McRoberts, L. D. Tisdale, and H. Masui. 1984. A human colonic tumor cell line that maintains rectorial electrolyte transport. *Am. J. Physiol.* 246:G204-G208.
20. Dharmasathaphorn, K., K. G. Mandel, H. Masui, and J. A. McRoberts. 1985. VIP-induced chloride secretion by a colonic epithelial cell line: direct participation of a basolaterally localized Na⁺, K⁺, Cl⁻ cotransport system. *J. Clin. Invest.* 75:462-471.
21. Field, M. 1981. Secretion of electrolytes and water by mammalian small intestine. In *Physiology of the Gastrointestinal Tract*. L. R. Johnson, J. Christensen, M. I. Grossman, E. D. Jacobson, and S. G. Schultz, editors. Raven Press, New York. 963-982.
22. Welsh, M. J., P. L. Smith, M. Fromm, and R. A. Frizzell. 1982. Crypts are the site of intestinal fluid and electrolyte secretion. *Science (Wash. DC)*. 218:1219-1221.
23. Cerejido, M., E. S. Robbins, W. J. Dolan, C. A. Rotunno, and D. D. Sabatini. 1978. Polarized monolayers formed by epithelial cells on a permeable and translucent support. *J. Cell Biol.* 77:853-880.
24. Handler, J. S., R. E. Steel, M. K. Sahib, J. B. Wade, A. S. Preston, N. L. Lawson, and J. P. Johnson. 1979. Toad urinary bladder cells in culture: maintenance of epithelial structure, sodium transport, and response to hormones. *Proc. Natl. Acad. Sci. USA*. 76:4151-4155.
25. Madara, J. L. 1983. Increases in guinea pig small intestinal transepithelial resistance induced by osmotic loads are accompanied by rapid alterations in absorptive cell tight junction structure. *J. Cell Biol.* 97:125-136.
26. Madara, J. L., M. R. Neutra, and J. S. Trier. 1981. Junctional complexes in fetal rat small intestine during morphogenesis. *Dev. Biol.* 86:170-178.
27. Montesano, R., D. S. Friend, A. Perrelet, and L. Orci. 1975. In vivo assembly of tight junctions in fetal rat liver. *J. Cell Biol.* 67:310-319.
28. Dawson, D. C. 1977. Na and Cl transport across the isolated turtle colon: parallel pathways for transmembrane ion movement. *J. Membr. Biol.* 37:213-233.
29. Freel, R. W., M. Hatch, D. L. Earnest, and A. M. Goldner. 1983. Role of tight-junctional pathways in bile salt-induced increases in colonic permeability. *Am. J. Physiol.* 245:G816-G823.
30. Pricam, C., F. Hunbert, and A. Perrelet. 1974. A freeze-etch study of the tight junctions of the rat kidney tubules. *Lab. Invest.* 30:286-291.
31. Sardet, C., M. Pisam, and J. Maetz. 1979. The surface epithelium of teleostean fish gills: cellular and junctional adaptations of the chloride cell in relation to salt adaptation. *J. Cell Biol.* 80:96-117.
32. Dziegielewska, K., C. A. N. Evans, D. H. Malinowska, K. Mollgard, J. M. Reynolds, M. L. Reynolds, and N. R. Saunders. 1979. Studies of the development of brain barrier systems to lipid insoluble molecules in fetal sheep. *J. Physiol. (Lond.)*. 292:207-231.
33. Olver, R. E., E. E. Schneeberger, and D. V. Walters. 1981. Epithelial solute permeability, ion transport and tight junction morphology in the developing lung of the fetal lamb. *J. Physiol. (Lond.)*. 315:395-412.
34. Mollgard, K., D. H. Malinowska, and N. R. Saunders. 1976. Lack of correlation between tight junction morphology and permeability properties in the choroid plexus. *Nature (Lond.)*. 264:293-294.
35. Duffy, M. E., B. Hamau, S. Ho, and C. J. Bentzel. 1981. Regulation of epithelial tight junction permeability by cyclic AMP. *Nature (Lond.)*. 204:451-453.
36. Bentzel, C. J., B. Hainau, S. Ho, S. W. Hui, A. Edelman, T. Anagnostopoulos, and E. L. Beneditti. 1980. Cytoplasmic regulation of tight-junction permeability: effect of plant cytokinins. *Am. J. Physiol.* 239:C75-C89.
37. Palant, C. E., M. E. Duffey, B. K. Mookerjee, S. Ho, and C. J. Bentzel. 1983. Ca²⁺ regulation of tight-junction permeability and structure in *Necturus* gallbladder. *Am. J. Physiol.* 245:C203-C212.
38. Metz, J., A. Aoki, M. Merlo, and W. G. Forssmann. 1977. Morphological alterations and functional changes of interhepato cellular junctions induced by bile duct ligation. *Cell Tissue Res.* 182:299-310.
39. Raviola, G., and E. Raviola. 1981. Paracellular route of aqueous outflow in the trabecular meshwork and canal of Schlemm. A freeze-fracture study of the endothelial junctions in sclerocorneal angle of the macaque monkey eye. *Invest. Ophthalmol. Vis. Sci.* 21:52-71.
40. Mazariegos, M. R., L. W. Tice, and A. R. Hand. 1984. Alteration of tight junctional permeability in the rat parotid after isoproterenol stimulation. *J. Cell Biol.* 98:1865-1877.
41. Marcial, M. A., and J. L. Madara. 1984. Osmotic disruption of the small intestinal macromolecular barrier: structure-functional analysis. *Gastroenterology*. 86:1172. (Abstr.)
42. Phillips, T. E., T. H. Phillips, and M. Neutra. 1984. Leakage of macromolecules through occluding junctions accompanies goblet cell secretion in intestinal crypts. *J. Cell Biol.* 99 (No. 4, Pt. 2):399a. (Abstr.)